Power Utility Maximization for Multiple-Supply Systems by a Load-Matching Switch

Chulsung Park and Pai H. Chou
Center for Embedded Computer Systems
University of California, Irvine, CA 92697-2625   USA
{chulsung,phchou}@uci.edu

ABSTRACT

For embedded systems that rely on multiple power sources (MPS), power management must distribute the power by matching the supply and demand in conjunction with the traditional power management tasks. Proper load matching is especially critical for renewable power sources such as solar panels and wind generators, because it directly affects the utility of the available power. This paper proposes a power distribution switch and a source-consumption matching algorithm that maximizes the total utility of the available power from these ambient power sources. Our method yields over 30% more usable power than conventional MPS designs.

Categories and Subject Descriptors

C.3.8 [**Computer Systems Organization**]: Special-Purpose and application-based systems—*Real-time and embedded systems*

General Terms

Design, experimentation

Keywords

Solar energy, photovoltaics, power model, solar-aware, power management, load matching

1. INTRODUCTION

A growing number of embedded systems has come to be known as multiple power source (MPS) embedded systems. As the name suggests, they rely on multiple power sources to replenish their energy over time for extended operations. Examples of these systems include satellite systems and sensor nodes. Satellites and some autonomous aircraft make extensive use of solar power, while sensor nodes may draw from other ambient energy sources such as wind and vibration. Because they must harvest energy from sources that are unstable and have a wide dynamic range, power management in MPS systems must consider power distribution and consumption together.
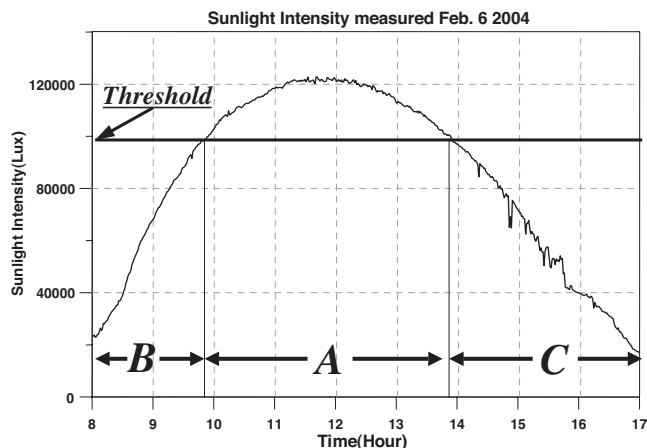
Figure 1: A typical solar power profile. Conventional systems can use only the energy in zone *A*, and zones *B* and *C* are wasted.

Today's MPS systems manage their power as follows. When the ambient source cannot supply power, the rechargeable battery must provide the power. The battery is recharged when the ambient sources can supply sufficient power. An important assumption is that the battery cannot be recharged and supply power at the same time. Instead, the supply power must be divided so that the entire system is powered on by the ambient source, while the remaining power goes to recharging the battery.

A problem with the conventional scheme is that much of the ambient power is wasted. This is because if the ambient power is not high enough to both drive the system and recharge the battery at the same time, then the battery must drive the system. Any power from the ambient source must be discarded in this case. As a result, these MPS systems must either use larger solar panels than necessary, or they operate for much shorter than optimal.

To illustrate this issue, consider a sensor node that must take 200 samples of vibration data and transmit them over a wireless link 24 hours a day. Its power sources consist of a solar panel and a rechargeable battery. The only time solar power can be utilized is zone *A* in Fig. 1, because that is when it can power up both the system and the rechargeable battery at the same time. During the other times, such as zones *B* and *C*, even though the output power is sufficiently high to drive either the entire system or at least some subsystems, the solar power must be discarded.

The goal of this paper is to maximize the utility of such power that otherwise would be wasted. This is accomplished with a new load-matching power switch that distributes the available power to the power consumers as much as possible. This has the potential of
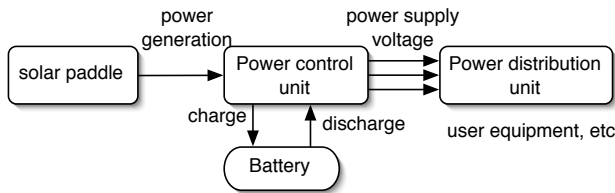
Figure 2: Power system of a satellite.

reclaiming 25%–50% of the power that would be wasted by conventional designs. By making more efficient use of the available power, the system can be designed to be more compact, operate for longer, and even slow down the aging process of batteries due to frequent recharge cycles.

2. RELATED WORK

This section surveys the power systems of existing MPS systems and the characteristics of the power sources.

2.1 Power systems of MPS

Many existing electronic systems already use multiple power sources. The most well-known MPS system is a satellite. As shown in Fig. 2, the satellite power system consists of the solar paddle, rechargeable batteries, the power control unit, and the power distribution unit [1, 2, 3, 4]. The power control unit regulates the output voltage of solar arrays using a DC/DC converter and controls charging and discharging of the battery. The power distribution unit is for distributing proper power to each subsystem. The Mars exploration rover [5] is another example of a MPS system. Its main power source is a multi-panel solar array, which can generates about 140 watts of power for up to four hours per *sol* (a Martian day). Its power system also includes two rechargeable batteries to supply power at night. One emerging MPS system is a wireless sensor node (WSN). Due to its limited size, a WSN cannot carry a battery of sufficient capacity for the entire mission. Therefore, researchers proposed energy renewing mechanisms from its environment of operation.

In all conventional designs listed so far, the battery cannot be recharged and discharged at the same time. As a result, the solar power can be utilized only if it is at least powerful enough to drive the system. Any excess power not utilized by the system is used to recharge the battery. When the available solar power drops below the minimum needed to drive the system, then the system switches to the battery as the power supply. We believe this scheme wastes significant amounts of solar energy, and this paper presents power distribution hardware and policies to utilize such power that would be wasted otherwise.

2.2 Characteristics of power sources

MPS systems use a variety of power sources with different characteristics. They often consist of one or more batteries plus renewable sources.

A battery is the most widely used power source in embedded systems, MPS or otherwise. Here, we consider mainly rechargeable ones for the ability to continue operation when other sources are not available. The chemistry of the battery determines its characteristics [6]. For instance, a NiCd battery has a high discharge rate (20C) and long cycle life (1500 charge/discharge cycles), but its energy density (45–80 Wh/Kg) and cell voltage (1.25V) are low. On the other hand, a Li-Ion or Li-Polymer battery has high energy density (110–160 Wh/Kg) and high cell voltage (3.6V), but
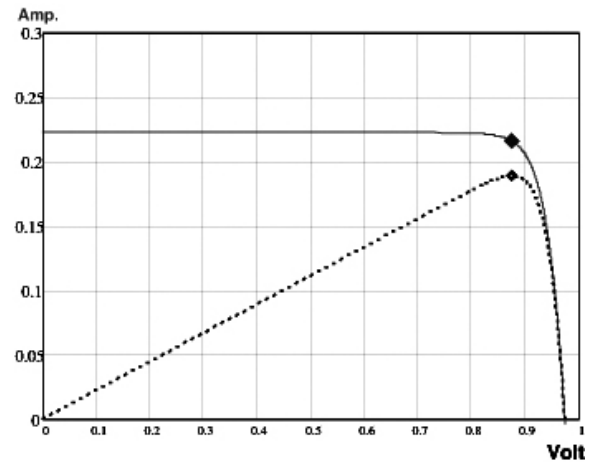
(Figure from Hansen [8])

Figure 3: I/V(solid line) and P/V(dotted line) characteristics of a typical GaAs solar cell. The maximum power point is marked by diamond.

comparatively low discharge rate (1C or lower) and short cycle life (300–500). A problem with these rechargeable batteries is that they suffer from degradation with use, due to memory effect and aging effect. Generally, fewer cycles and less charge taken out in each cycle lead to a longer battery life. A battery also has a relaxation effect, where a "rest" is beneficial for the battery. Discharging a battery at high discharge rates continuously results in reduced lifetime, because the energy still in the battery becomes inaccessible.

A solar panel has totally different characteristics from batteries [7]. It is a renewable power source. However, since the sunlight intensity is not always constant, its power output has a wide dynamic range. Even though the sunlight intensity is almost constant within a short time interval, because a solar cell behaves like a current source with a voltage limiter, it is very important to operate the load at the maximum-power point. Fig. 3 shows the maximum point at a given sunlight intensity [8]. The conversion efficiency depends on the material of solar cell, but it is at most 25% and is relatively low.

A wind generator is another potential power source for MPS systems [9, 10]. Currently, most wind generators are vertical types and are designed to generate high power. These large wind generators may not be applicable to small MPS systems, but recently smaller, high efficiency ones can be a good power source. Depending on the location, it may be difficult to predict how much power will be generated. Therefore, it may be more appropriate to use a wind generator as an instant power source for bulk data transmission.

Other potential power sources such as vibration, temperature difference, and acoustic noise are under research [11, 12, 13]. However, because the power level they can generate is extremely low, they are currently used only in exceptional or experimental systems.

3. PROBLEM STATEMENT

The goal is to maximally utilize the ambient power that would otherwise be wasted, as illustrated in zones *B* and *C* in Fig. 1 earlier. To achieve this, we need (1) the *mechanisms* for tracking the available power level and "routing" power from multiple source to multiple subsystems, and (2) power management *policies* to go with
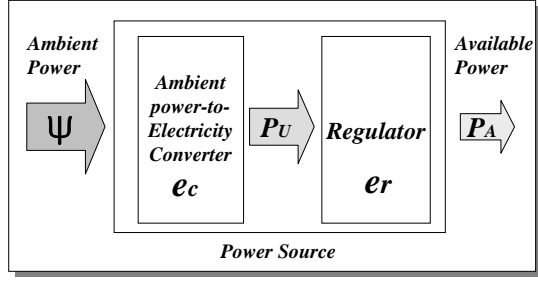
Figure 4: Model of Power Source.

these mechanisms. This section present the power source model, problem formulation, and an algorithm for policy generation.

Fig. 4 shows the power source consisting of an ambient power-to-electricity converter and a voltage regulator. A converter such as a solar panel and wind generator generates *unregulated power* P_U with the *conversion efficiency* e_c from the ambient power, whose *intensity* is Ψ.

$$P_U = e_c \cdot \Psi \qquad (1)$$

To step up or down the output voltage of this converter, we use a voltage regulator whose *regulation efficiency* is e_r, and thus the *available power* P_A on the power source is

$$P_A = e_r \cdot P_U = e_r e_c \cdot \Psi \qquad (2)$$

The problem statement is given as follows. Given the following:

(a) An MPS system consisting of

  $m-1$ ambient power sources and one rechargeable battery $G = \{g_i | 1 \le i \le m\}$, where $g_1 \ldots g_{m-1}$ are ambient power sources and g_m is the rechargeable battery, and

  $n-1$ subsystems and one battery charger $S = \{s_j | 1 \le j \le n\}$, and s_n is the battery charger

(b) The available power p_{A_i} on each power source g_i.
   $P_A = \{p_{A_i} | 1 \le i \le m\}$

(c) The power consumption p_{C_j} by each subsystem s_j.
   $P_C = \{p_{C_j} | 1 \le j \le n\}$

We define the following:

(d) The *connection matrix C*, which indicates the connection between g_i and s_j, and whose elements are c_{ij}, where $c_{ij} \in \{0,1\}$, for $1 \le i \le m-1, 1 \le j \le n$.

(e) The *power demand* p_{D_i} on each power source g_i.
   $P_D = \{p_{D_i} | 1 \le i \le m\}$

$$p_{D_i} = \sum_{j=1}^{n} c_{ij} p_{C_j} \qquad (3)$$

The problem is to find a connection matrix C to maximize

$$\sum_{i=1}^{m-1} p_{D_i} = \sum_{i=1}^{m-1} \sum_{j=1}^{n} c_{ij} p_{C_j} \qquad (4)$$

under the conditions of

a) power demand should not exceed the available power:

$$
\begin{aligned}
p_{A_1} &\ge p_{D_1} &=& \quad c_{11}p_{C_1} + c_{12}p_{C_2} + \ldots + c_{1n}p_{C_n} \\
p_{A_2} &\ge p_{D_2} &=& \quad c_{21}p_{C_1} + c_{22}p_{C_2} + \ldots + c_{2n}p_{C_n} \\
p_{A_3} &\ge p_{D_3} &=& \quad c_{31}p_{C_1} + c_{32}p_{C_2} + \ldots + c_{3n}p_{C_n} \\
& & & \ldots \\
p_{A_m} &\ge p_{D_m} &=& \quad c_{m1}p_{C_1} + c_{m2}p_{C_2} + \ldots + c_{mn}p_{C_n}
\end{aligned}
\qquad (5)
$$

b) one subsystem can be connected to only one power source:

$$\sum_{i=1}^{m-1} c_{ij} = 1 \quad \text{for } j = 1, \ldots, n-1 \qquad (6)$$

c) the battery charging subsystem can be connected to the power source only after all other subsystems are already connected to power sources:

$$\sum_{j=1}^{n-1} \sum_{i=1}^{m-1} c_{ij} = n-1 \quad \Rightarrow \quad \sum_{i=1}^{m-1} c_{in} = 1 \qquad (7)$$

This is a bin-packing problem and is NP-complete in the general case. However, for many systems, we cannot arbitrarily turn on or turn off individual subsystems due to system-level dependencies. Instead, the number of system-level power configurations to consider is rather small. The available power value p_{A_i} from each source is mapped to a digit $q(p_{A_i})$, and the digits are concatenated to form a number x that is used to index into a table of configurations Γ. Each entry $\gamma \in \Gamma$ specifies a connection matrix that maximizes the expression in Eqn. (4), and the satisfaction of Eqns. (5), (6), (7) are checked at compile time. At runtime, managing the load-matching switch can be made very simple.

FINDCONFIG(P_A, Γ)

  $\triangleright$ looks up a statically computed configuration at run time
  $\triangleright$ based on power availability from different sources
1   $x \leftarrow \langle q(p_{A_1}), \ldots, q(p_{A_m}) \rangle$
2   **return** $\Gamma[x]$

4. POWER UTILITY MAXIMIZER (PUMA)

In this section, we propose the *power utility maximizer* switch, called PUMA, to maximize utilization of power sources. We also show how to apply PUMA to an actual MPS embedded system.

4.1 The PUMA Hardware

PUMA is to maximize the utility of power sources by matching load to available power. PUMA senses the available power on each power source and find a connection scheme between subsystems and power sources to maximize the utilization. Fig. 5 shows a PUMA consisting of sensors, switch array, and the controller. Sensors are to measure the intensity of ambient energy such as sunlight intensity, wind speed, and vibration. Those measured data are sent to the controller and used to calculate the available power on each source. The controller runs the algorithm or refers to look-up table to get the connection matrix C to maximize the utilization of power sources. Finally, it sends the connection matrix to the switch array, which establishes the connections between the power sources and the subsystems.

Fig. 6 shows the switch unit of PUMA. Each switch unit has one power path controller (LTC4412) and as many PMOS switches (MIC94060) as power sources. The power path controller is for smoothing transitions between the battery and other power sources, and the PMOS switches physically establish the connections between the power sources and the subsystems according to the PUMA
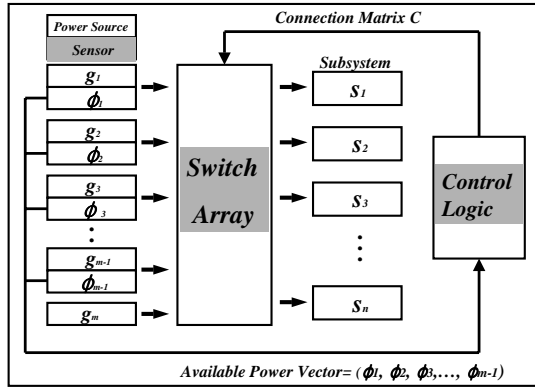
Figure 5: The block diagram of the PUMA (power utility maximizer) switch.
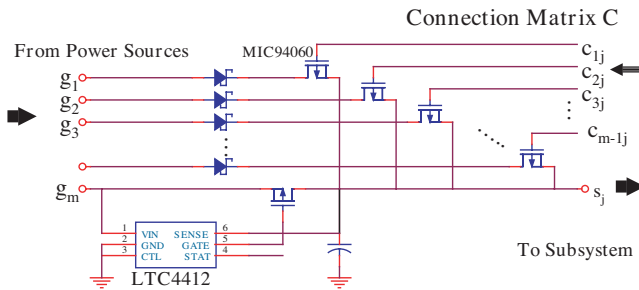

Figure 6: Schematic of the PUMA switch unit.

controller. The PUMA switch array consists of as many switch units as the subsystems.

4.2 Implementation Example: DuraNode

We applied PUMA to an actual MPS embedded system called DuraNode, a wireless sensor node for real-time structural health monitoring. As shown in Fig. 7, DuraNode consists of three individual boards: wireless communication board, microcontroller and sensor board, and the power system board. Fig. 8 shows the block diagram of DuraNode. Its two power sources consist of a rechargeable battery and a solar panel, and its four subsystems are the microcontroller, sensor devices (ADXL and SD accelerometers), the wireless card (802.11b), and the battery charger. Its microcontroller (PIC18F6680) samples vibration from two accelerometers and sends them to the host computer via the 802.11b wireless LAN interface. Before applying PUMA, the power system of DuraNode had only one switch unit, and thus it was able to select one power
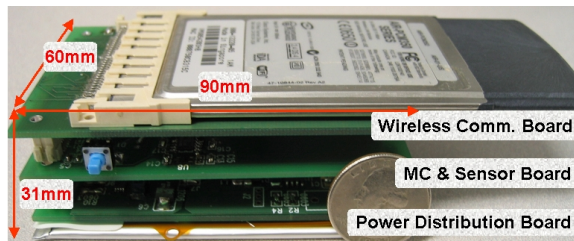

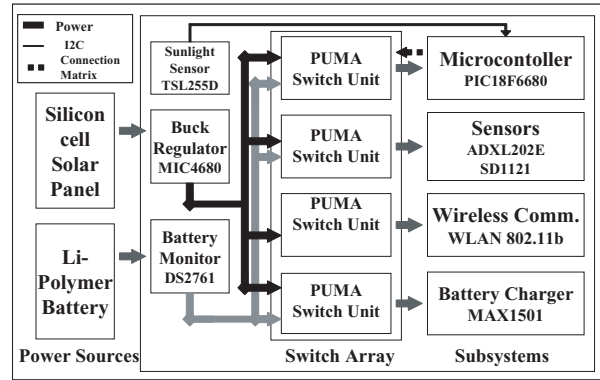**Figure 7: A photo of the DuraNode wireless sensor system.**

Figure 8: Application of PUMA to the power system of Dura-Node.

Mode	Connection		Lux
	Battery	Solar Panel	
M0	M, S, W		
			121
M1	S, W	M	
			435
M2	M, W	S	
			477
M3	W	M, S	
			773
M4	M, S	W	
			813
M5	S	M, W	
			942
M6	M	S, W	
			979
M7		M, S, W	
			1123
M8		M, S, W, B	

M: Microcontroller subsystem   S: Sensor subsystem
W: WLAN 802.11b subsystem   B: Battery Charging subsystem

Table 1: Lookup Table.

source at a time between the battery and the solar panel. In other words, DuraNode had only two power mode: in M_0, all subsystems are powered by the battery; in M_1, all subsystems are powered by the solar panel.

To apply PUMA, we modified the power system by adding a sunlight intensity sensor (TSL2550) and the switch array. The array has four switch units, as shown in Fig. 8. This modification enables DuraNode to have nine power modes, as shown in Table 1. DuraNode first computes the available power on the solar panel based on the sunlight intensity measured by the light sensor. Then, the lookup table maps the sunlight intensity to the best power mode, which enables the solar panel to power as many subsystems as possible.

5. EXPERIMENTAL RESULTS

5.1 Experimental Setup

Fig. 9 shows our experimental setup. The DuraNode is programmed to sample vibration along the X, Y, and Z axes, to sample sunlight intensity, and to send the data to the host computer over UDP. The transmission speed is set to the full 11Mbps speed of 802.11b, and the data size for each transmission is 60 bytes. The solar panel has a fixed orientation facing south at $75°$ from the
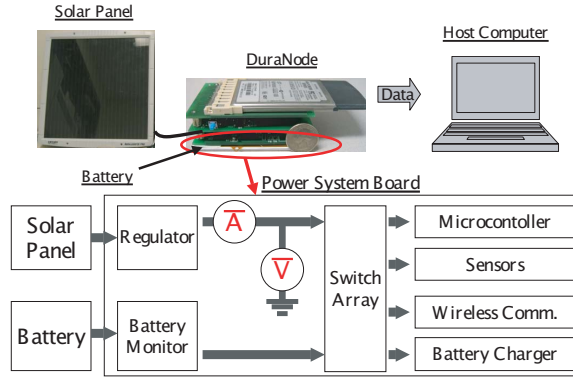
Figure 9: The experimental setup with DuraNode.

Subsystem	Power
Microcontroller	67.5mW
Sensor	421mW
WLAN 802.11b	1125mW
Battery charging	450mW

Table 2: Power Consumption of each subsystem

ground. The sunlight intensity sensor of the DuraNode is placed at the center of the solar panel. To measure the power drawn from the solar panel, we connect an ampmeter in series and a voltmeter in parallel between the regulator of the solar panel and the Dura-Node. Our measurement was conducted for 9 hours, from 8:00am to 5:00pm on January 6, 2004. We measured the power consumption of each subsystem shown in Table 2. We also measured the sunlight intensity level for each power mode to make a lookup table, shown in Table 1.

5.2 Results

Fig. 10 shows the profile of the available power on the solar panel and the power consumption profile by the DuraNode. The available power on the solar panel is calculated from the sunlight intensity data measured by the sensor. (1000Lux = 0.021Watts @33cm^2 silicon cell solar panel). The power drawn by the DuraNode is calculated by multiplying the measured voltage and current values. The

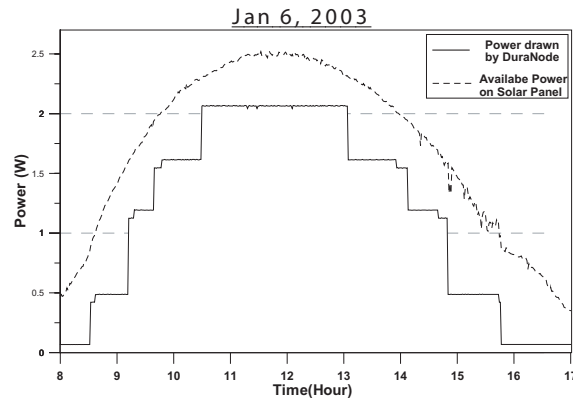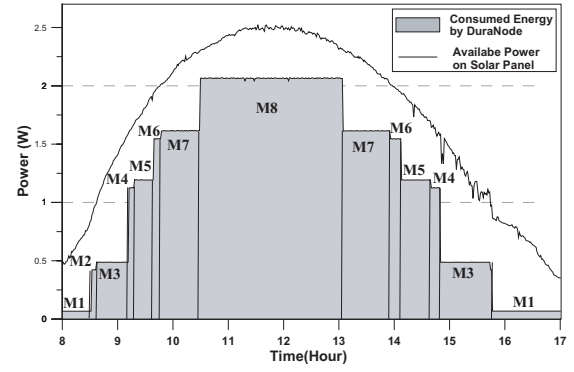**Figure 10: Available power on solar panel and power drawn by DuraNode.**

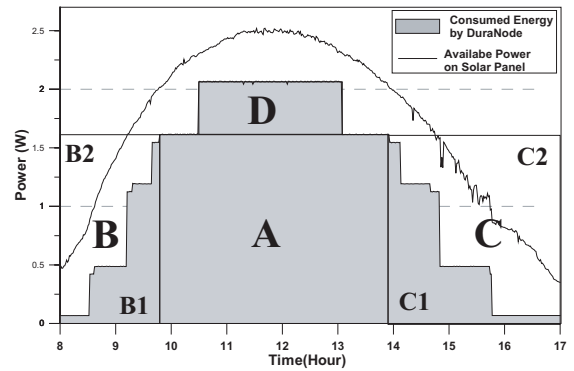**Figure 11: Power mode of DuraNode tracking the sunlight intensity**

Figure 12: Energy zones of DuraNode

gap between the solid and dotted graph represents the power loss due to the regulator (regulation efficiency $e_r < 1.0$) and, more significantly, the mismatch between the load and the optimal power output level of the solar panel.

In Fig. 11, we observe that the power mode of DuraNode tracks changes in the sunlight intensity. At 9:47am, the sunlight intensity first exceeds the threshold for powering the entire system. So, DuraNode sets its power mode to $M7$. At 10:29am, DuraNode enters mode $M8$ in which the solar panel also charges the battery.

In Fig. 12, we divide the graph into four zones. In zone A, the solar panel can solely power the entire system, and thus the area represents the energy drawn from the solar panel. In zones B and C, the solar power is not high enough to power the entire system, and DuraNode is powered by both the battery and the solar panel. The gray areas B_1 and C_1 represent the energy from the solar panel, whereas the white areas B_2 and C_2 represent the energy from the battery. In zone D, the area represents the portion of the solar energy allocated for charging the battery. Therefore, the total energy drawn from the solar panel is

$$E_S = E_A + E_{B1} + E_{C1} + E_D \qquad (8)$$

and the energy from the battery is

$$E_B = E_{B2} + E_{C2} \qquad (9)$$

In contrast, the conventional MPS system must be powered by only the battery in zones B and C. Therefore, the energy from the solar panel reduces to $E'_S = E_A + E_D$ and the energy from the battery will
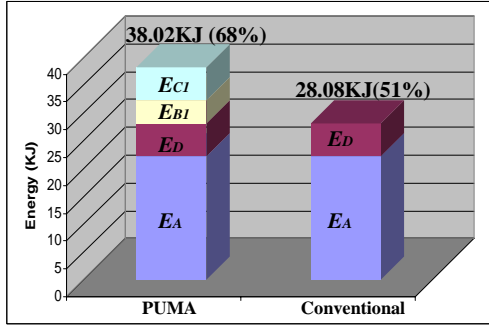
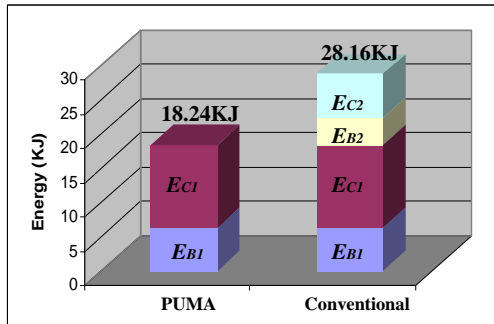**Figure 13: Comparison: Utilization of the solar energy**

Figure 14: Comparison: Energy drawn from the battery

increase to $E'_B = E_B + E_C$. In our experiment, $E_S = 38.02$KJ, $E_B = 18.24$KJ, $E'_S = 28.08$KJ, and $E'_B = 28.16$KJ. Also, the total energy available on the solar panel is $E_T = 55.75$KJ.

Fig. 13 compares the utilization of the solar energy. The solar power utilization of PUMA is $E_S/E_T = 68\%$, whereas the conventional system is $E'_S/E_T = 51\%$. In other words, PUMA extracts $(E_S - E'_S)/E'_S = 33\%$ more energy from the same source. In terms of absolute energy, PUMA consumes 9.92KJ less than the conventional system, as shown in Fig. 14.

6. CONCLUSIONS

This paper presents a novel technique for matching the power sources and power consumers. This is accomplished through a combination of the PUMA hardware switch and the power configuration policy. Our technique effectively increases the utilization of the ambient power that would otherwise be wasted. Because power is a precious resource in these MPS embedded systems, increasing the utility will be the most important step towards the optimization and extended operation of this important class of low-power embedded systems.

Acknowledgments

7. REFERENCES

[1] D. Loche, J.-M. Dubouch, and A. Lehmann. Power system for LEOSTAR^{TM}. In *Proceedings of the Fifth European Space Power Conference*, 1998.

[2] Dermott O'Sullivan. Satellite power system topologies. *ESA Journal*, 13:77 – 88, 1989.

[3] J.E. Haines. European LEO spacecraft power systems... what's next? In *Proceedings of the European Space Power Conference*, 1993.

[4] NASDA (National Space Development Agency of Japan). *Report Research on Small, Lightweight Satellite Power System to Improve Mission Performance*, (123), September 2003.

[5] The rover's energy. `http://marsrovers.jpl.nasa.gov/mission/spacecraft_rover_energy.html`.

[6] David Linden and Tomas Reddy. *Handbook of Batteries*. McGraw-Hill, 2001.

[7] Jeff Bailey, Scott A. McHugo, Henry Hieslmair, and Eicke R. Weber. Efficiency-limiting defects in silicon solar cell material. *Journal of Electronic Materials*, 25(9):1417 – 1421, September 1996.

[8] Flemming Hansen. Electrical power system architecture for small scattersite. `http://www.dsri.dk/dssp/EPS_Smallsat_Architecture.pdf`.

[9] Tönics Peets, Andres Annuk, Veli Palge, and Jaan Lepa. Modeling of characteristics of small scale wind unit. `http://tehnika.eau.ee/pages/2002/Energy/33_Peets_Annuk_Palge_Lepa.pdf`.

[10] The energy development co-operative web page Aerogen wind generator technical specification. `http://www.unlimited-power.co.uk/Aerogen_spec.html`.

[11] Scott Meninger, Jose Oscar Mur-Miranda, Rajeevan Amirtharajah, Anantha Chandrakasan, and Jeffrey Lang. Vibration-to-electric energy conversion. In *Proceedings of the 1999 international symposium on Low power electronics and design*, August 1999.

[12] S. Roundy, B. Otis, Y.H. Chee, J. Rabaey, and P. Wright. A 1.9GHz RF transmit beacon using environmentally scavenged energy. In *Dig. IEEE Int. Symposium on Low Power Elec. and Devices*, 2003.

[13] Aman Kansal and Mani B. Srivastava. An environmental energy harvesting framework for sensor networks. In *International Symposium on Low Power Electronics and Design*, 2003.